

The Quasi-Biennial Oscillation: Analysis using ERA-40 data

Charlotte L. Pascoe ¹

Lesley J. Gray ²

Simon A. Crooks ³

Martin N. Jukes ¹

Mark P. Baldwin ⁴

1. Rutherford Appleton Laboratory, UK
2. Centre for Global Atmospheric Modelling, Reading University, UK
3. Oxford University, UK
4. North West Research Associates, USA

Abstract

The ERA-40 data set is used to examine the equatorial quasi-biennial oscillation (QBO). The data set extends from the ground to 0.1 hPa (~65 km) and covers a 44 year period (January 1958 to December 2001), including 18.5 QBO cycles. Analysis of this data set of unprecedented spatial and temporal coverage has revealed a 3-fold structure in height in the QBO zonal wind anomalies at the equator. In addition to the well-known 2-fold structure in the lower and mid stratosphere, i.e. easterlies overlying westerlies or vice versa, there is a third anomaly in the upper stratosphere. The sign of this upper stratospheric anomaly is the same as the lower stratospheric anomaly, thus forming anomalies of alternating sign throughout the depth of the equatorial stratosphere. The amplitude of this upper stratospheric anomaly is ~10 m/s, approximately 1/3 of the amplitude of the lower stratospheric signal. The frequency and descent rates of the east and west QBO phases are analysed in detail, with particular attention to any 11-year solar cycle influence. In addition to the observed solar modulation of the duration of the QBO west phase, the analysis shows a solar modulation of the mean descent rate of the easterly shear zone. The mean time required for the easterly shear zone to descend from 20 hPa to 44 hPa is 2 months less under solar maximum conditions than under solar minimum conditions (7.4 months versus 9.7 months). This rapid descent of the easterly shear zone cuts short the west phase of the QBO in the lower stratosphere during solar maximum periods.

1. Introduction

The equatorial stratosphere is dominated by downward propagating easterly and westerly zonal wind regimes. This oscillating pattern of equatorial winds was discovered by *Ebdon* (1960) and *Reed et al.* (1961) and later became known as the quasi-biennial oscillation, or QBO (*Angell and Korshover*, 1964). The basic physical mechanisms of the phenomenon were explained by *Holton and Lindzen* (1972). An excellent description of the current understanding of the quasi-biennial oscillations of wind, temperature and ozone can be found in *Baldwin et al.* (2001).

In this paper we use the new ERA-40 dataset (described in section 2) to update the work of *Baldwin et al.* (2001). In section 3 we present a Fourier analysis of the equatorial zonal mean zonal wind. In section 4 we diagnose general QBO diagnostics and present evidence of a three-fold vertical QBO phase structure. In section 5 we look at the variability of the QBO and examine the possibility of a modulation of the QBO by the solar cycle. A summary of the results is presented in section 6.

2. The ERA-40 dataset

A new synthesis of in-situ and remotely-sensed measurements for the period since mid-1957 has been employed in this study. It was prepared by ECMWF (European Centre for Medium Range Weather Forecasting) using their variational data assimilation system and is referred to as the ERA-40 dataset (<http://www.ecmwf.int/research/era>). Apart from the obvious extended length of the ERA-40 dataset compared with the earlier ERA-15 dataset, an important difference is in the use of satellite data. ERA-40 includes the TOVS (TIROS Operational Vertical Sounder) radiances directly, while in ERA-15 retrievals of temperature and humidity were used. A second important difference is in the vertical

extent of the dataset. The ERA-40 data coverage extends to 0.1 hPa compared with ERA-15 that extended to 10 hPa only.

In addition to the traditional data used in the assimilation such as radiosonde observations, VTPR (Vertical Temperature Profile Radiometer), TOVS and CMW (Cloud Motion Winds) satellite observations were used in the period 1972-1988 and TOVS, SSM/I (Sensor Microwave Imager), ERS (European Remote Sensing Satellite), ATOVS (Advanced Tiros Operational Vertical Sounder) and CMW satellite observations were used in the period 1987-2001. Post-1979 TOVS consisted of SSU/HIRS/MSU, plus AMSU/HIRS from 1998 onwards. The SSU and AMSU observations are predominant at upper stratospheric levels.

The ERA-40 dataset consists of 6-hourly analyses throughout the period 1957-2001. The data are of high spatial resolution, with a grid-spacing close to 125 km in the horizontal (T159) and with 60 levels in the vertical located between the surface and 0.1 hPa (approximately 65 km). The data are available on 23 standard pressure surfaces from the surface to 1 hPa. Data are also available on model levels. All figures shown in this paper were prepared using the monthly-averaged data from the 6-hourly analyses on standard pressure surface data up to 100 hPa. Above that level the model level data were used to extend the figures to 0.1 hPa. However, caution is required in the interpretation of data above 1 hPa (approximately 50 km) since this will be contaminated by the close proximity of the top of the model.

The ERA-40 analyses provide a good representation of the QBO, as judged by comparisons with wind observations and independent analyses. We note that the ERA-40 analysed temperatures in the upper stratosphere are sensitive to the availability and use of

satellite measurements. In particular, the semi-annual oscillation (SAO) increases in magnitude with the onset of the assimilation of TOVS irradiances in 1979. For this reason we use data only for the period 1979 – 2001 for some of the analysis, because of the improved irradiance data that were assimilated in that period. Abrupt changes in upper stratospheric temperature can also be found where adjacent data streams meet. However, this feature appears to significantly affect only the temperatures and not their latitudinal gradients; the zonal wind time-series does not suffer significantly from these abrupt changes (see figure 1).

3. The Equatorial QBO

The time-series of monthly-averaged, zonally-averaged zonal winds for the complete ERA-40 dataset 1958 – 2001 is shown in figure 1(a). A comparison with the corresponding time-series of radiosonde data (*Naujokat* 1986) and rocketsonde data (*Gray et al.* (2001b) show that the QBO is captured extremely well by the ERA-40 dataset. The alternating easterly and westerly winds are the dominant feature of the climatology of the stratosphere between 5-100 hPa. The different descent rates of the easterly and westerly shear zones can be clearly seen, and the marked ‘stalling’ of the easterlies in certain years, for example in 1965 and 1989 is evident. Above 5 hPa the time-series is dominated by the semi-annual oscillation (SAO). When the annual cycle is removed (figure 1b) and the data are passed through a broad-band 9-48 month digital filter (figure 1c) the SAO is effectively removed and the QBO signal can be seen to extend as high as 1 hPa, although its amplitude is reduced to around $\pm 5-10 \text{ ms}^{-1}$.

The mean annual cycle of equatorial zonal mean zonal wind for the period 1979-2001 is shown in figure 2. The 1979-2001 interval was chosen because of the improved satellite irradiance data that was assimilated in that period. Figure 2 clearly shows the regular semi-annual oscillation above 35 km and the annual modulation of the amplitude of the SAO which is strongest during northern hemisphere winter. The maximum easterlies reach -38 ms^{-1} and the maximum westerlies reach $+20 \text{ ms}^{-1}$ in the region of the stratopause ($\sim 1 \text{ hPa}$) during northern hemisphere winter-spring. The corresponding amplitudes in the second SAO phase are -18 ms^{-1} and $+10 \text{ ms}^{-1}$ respectively. This compares well with that found by *Swinbank and O'Neill* (1994). In addition to the asymmetry in magnitude there is also an asymmetry in the depth to which the westerly phase of the SAO penetrates. It is the weaker westerly SAO that penetrates most deeply into the stratosphere during November and December, when zonal mean westerlies extend on average down to 35 km.

In the lower stratosphere and troposphere the ERA-40 annual cycle also compares well with the NCEP reanalysis data presented by *Huesmann and Hitchman* (2001). Both show an easterly maximum in the upper troposphere during northern hemisphere summer which has been associated with the Tibetan high (*Hitchman et al.*, 1997), and also a time mean easterly wind shear which increases with height in the lower stratosphere up to 10 hPa.

3.1. Fourier Analysis of Equatorial Zonal Wind

The ERA-40 equatorial zonal mean zonal wind data has been passed through a Fourier filter in order to isolate the major periodic modes of variability. The Fourier frequency analysis was performed for each model level and the spectrum of periodic modes which were obtained mapped onto the frequency-height plot shown in figure 3. Fourier analysis

expects data which is either stationary or periodic and linear, when this is not the case one can expect the Fourier peaks to become broader.

The most frequent and distinct mode of variability to be found is the semi-annual oscillation (SAO) which completed 88 cycles during the 44 years of the ERA-40 record. The SAO is present in the upper stratosphere and mesosphere above 35 km. The next mode of variability at 44 cycles is the annual cycle. The annual signal is present in the upper troposphere and stratosphere and the maximum frequency response lies near the stratopause at 45 km where it modulates the amplitude of the SAO (figure 2), as already discussed.

Unlike the annual and semi-annual cycles, the frequency of the QBO varies throughout the ERA-40 time series. Hence the Fourier analysis is unlikely to see a strong spike at any particular frequency but rather a broad area of QBO side-bands. The asymmetry between the amplitudes and rates of descent of the east and west phases of the QBO will also contribute to the broadness of the harmonic response. Figure 3 shows the broad QBO frequency range lying between 13 and 24 cycles, corresponding to periods of 40 and 22 months respectively. However, within the amorphous QBO zone a distinct maximum can be seen between 18 and 19 cycles which together indicate a QBO period of approximately 28.5 months. Vertically the QBO frequencies extend throughout the depth of the stratosphere from 18 km to 50 km.

The Fourier spectrum in figure 3 also reveals a harmonic response at 4 cycles, which corresponds to a period of 11 years, extending between 25 and 40 km. It seems plausible that this zonal wind oscillation could be a response to the 11 year solar cycle.

4. QBO Diagnostics

Here we investigate the amplitude, period and vertical phase structure of the QBO in the ERA-40 dataset. We also examine the relationship between equatorial QBO wind shear and temperature anomalies.

4.1. QBO Amplitude

The Fourier analysis of the equatorial zonal mean zonal wind displayed in figure 3 found a broad spectrum of QBO frequencies between 13 and 24 cycles corresponding to QBO periods of 40 and 22 months respectively. To assess the contribution that the QBO makes to the overall variability in the zonal wind the ratio of the power spectrum of the QBO to the power spectrum of the entire ERA-40 dataset has been calculated. That is, the sum of the squares of the amplitudes of the QBO harmonics divided by the sum of the squares of the amplitudes of all harmonics. This yields a maximum QBO contribution of 81% centred near the equator at 20 hPa. The QBO ratio can then be multiplied by a measure of the amplitude of zonal wind variability (given by $\sqrt{2}$ times the root mean square of the zonal wind) to yield an objective evaluation of the amplitude of the QBO.

Figure 4a shows a latitude cross-section of the amplitude of the QBO in ms^{-1} calculated using the Fourier technique described above. QBO zonal winds are present over the equator from 20°S to 20°N and throughout the depth of the stratosphere from 100 to 1.0 hPa. The maximum QBO amplitude of 22.5 ms^{-1} is centred on the equator at 15-20 hPa. Figures 4b) and 4c) compare the amplitude of the QBO calculated using Fourier analysis with the Equivalent QBO Amplitude (EQA) which is defined by Randel *et al.* (2002) as $\sqrt{2}$ times the root mean square of the deseasonalised zonal wind. The Fourier method produces a maximum QBO amplitude that is 5.4 ms^{-1} smaller than the EQA, yet both methods reach a maximum QBO amplitude at $\sim 30 \text{ km}$ (20 hPa). It is possible that the

discrepancy in QBO amplitude at this altitude is due to leakage from the Fourier peak. However, above 35 km (7 hPa) the two QBO profiles diverge significantly. Fourier analysis of the deseasonalised equatorial winds (not shown) reveals the presence of significant amplitudes at annual and semi-annual periodicities above 35 km (7 hPa). Since deseasonalisation does not completely remove all high frequency harmonics, the variability captured by the EQA above 35 km must inevitably be an overestimation of the true QBO amplitude.

4.2 QBO Period

The mean period of the ERA-40 QBO has been established by timing the interval between successive occurrences of zero zonal mean zonal wind. This method yields a mean QBO period of 28.4 months which is marginally longer than the 28.2 months measured by *Baldwin et al.* (2001) and the 27.7 months obtained by *Naujokat* (1986). The standard deviation of the ERA-40 QBO is 4 months. Applying the Student's T-test to the ERA-40 data yields a 95% confidence interval of 28.4 ± 1.98 months. This 95% confidence range encompasses all of the other quoted measurements of QBO period so we can conclude that there is no significant difference between them.

4.3 QBO Vertical Phase Structure

Figure 5 yields information about the vertical phase structure of the QBO. It shows composites of the zonal mean zonal wind for the east and west phases of the QBO together with their difference. The QBO phase was classified according to the mean equatorial zonal mean zonal wind at 44hPa for the months of December and January. QBO west years are where this mean exceeds $+5 \text{ ms}^{-1}$ and QBO east years where the mean is less than -5 ms^{-1} . Transition years where the mean value fell between $\pm 5 \text{ ms}^{-1}$

were excluded. The west composite (figure 5a) is made up of 19 years and the east composite (figure 5 b) of 17 years (see table 1).

Figure 5 confirms the area of the QBO perturbation found by the Fourier analysis described above by showing that QBO zonal wind anomalies dominate the entire tropical stratosphere. This is particularly clear in the difference plot, figure 5c, where the student's T-test shading shows that the difference between the means of the two QBO phase regimes is significant to a confidence of 95% throughout the breadth of the tropics and the depth of the stratosphere.

The difference plot (figure 5c) also highlights a three-fold vertical phase structure of the QBO zonal wind anomalies. The west minus east difference is positive in the lower stratosphere centred about 23 km ($+30 \text{ ms}^{-1}$), negative in the mid-stratosphere centred about 35 km (-25 ms^{-1}) and then positive in the upper stratosphere centred about 48 km ($+10 \text{ ms}^{-1}$). This three-fold phase structure of the QBO can also be discerned from the deseasonalised QBO time series shown in figure 1b. The slow rate of descent of each QBO phase is such that a new phase is present in the upper stratosphere while an earlier phase of the same sign lingers on in the lower stratosphere. Sandwiched between these is a QBO phase of the opposite sign thus yielding the three-fold phase structure described above. The three-fold QBO structure can also be found in the tropical rocketsonde data displayed in figure 6 of *Gray et al. (2001b)*. The presence of the upper level QBO anomaly was also utilised by *Gray et al. (2001a)* to improve their model simulation of the extra-tropical QBO signal.

However, in general the third phase of the QBO in the upper stratosphere has either not been captured or has been ignored by previous authors/studies. *Randel et al. (1999)* made

an analysis of 7 years of (UK Met Office) UKMO stratospheric analyses and noted that the QBO had a continuous signal that could be traced as high as the stratopause and that the winds there were out of phase with those at 30 km. This implies a three fold QBO phase structure since the zonal wind at 30km also tends to be out of phase with winds in the lower stratosphere. A three fold structure was also clearly present in their figure 8 which showed a latitude-height time series of QBO zonal wind anomalies. Yet no note was made of the third QBO phase in the text except to state that the QBO zonal wind anomalies in the upper stratosphere are of the same magnitude as the residual. *Swinbank and O'Neill* (1994) assessed the ability of the UKMO model (used by *Randel et al.* (1999)) to capture the QBO and found that the decay of the QBO amplitude above 10hPa was too rapid in the UKMO analyses. *Swinbank and O'Neill* (1994) also noted problems associated with the lack of direct wind measurements above 10 hPa which meant that the assimilation system was unable to resolve shear zones fully. It therefore seems logical, given the reservations over the accuracy of the UKMO model in the upper stratosphere, that *Randel et al.* (1999) did not emphasise the third QBO phase.

The National Meteorological Centre (NMC) analyses used by *Baldwin and Dunkerton* (1991) have an upper limit in the region of the stratopause at 1hPa ~50km but showed only at two-phase vertical QBO structure. These analyses were also used as the basis of the QBO schematic in *Baldwin et al.* (2001) – see their plate 2. The magnitude of the equatorial QBO zonal winds in the NMC analyses is only about one third of that measured at the Singapore radiosonde station as a result of cross-equatorial interpolation (*Baldwin and Dunkerton*, 1991). This suggests that the dataset has insufficient resolution and quality to resolve the smaller QBO anomaly in the upper stratosphere.

Other models such as the National Centre for Environmental Prediction (NCEP) analyses and ERA-15 are only able to capture a 2-fold QBO structure because the top of the model is at 10hPa and is therefore too low to see the third QBO phase.

4.4 QBO Wind Shear and Temperature

In the tropics where the Coriolis parameter is small the thermal wind relationship nevertheless holds in the lower stratosphere because the equatorial QBO wind variations have a long time scale and are symmetrical about the equator (*Tanii and Hasebe, 2002*). Therefore westerly vertical shear in the zonal wind is associated with warm temperature anomalies at the equator and easterly vertical shear with cold anomalies.

Figure 6 displays the equatorial zonal mean deseasonalised temperature anomalies at 30 hPa and the zonal mean vertical wind shear in the 30 to 55 hPa layer. The two parameters are in phase which is to be expected since the tropical temperature QBO is in thermal wind balance with the vertical shear in the zonal wind. The equatorial QBO temperature anomalies which are of the order of ± 4 K are consistent with the 30 hPa Singapore Radiosonde temperatures noted by *Baldwin et al. (2001)*.

A note-worthy exception to the close link between lower stratospheric temperatures and the zonal wind shear can be seen in 1991 when there is a sudden increase in temperature which is not partnered by a change in the shear of the zonal mean wind. The sudden 4 K temperature increase is coincident with the eruption of Mount Pinatubo ($15^{\circ}\text{N}, 120^{\circ}\text{E}$) on June 14th / 15th 1991. The Pinatubo eruption created a cloud of stratospheric aerosol that circled the globe within two weeks and spread throughout the tropics between 20°S and 30°N (*McCormick and Veiga, 1992*). In the stratosphere the sulphate gases injected by large volcanic eruptions convert to sulphate aerosols with an e-folding residence time of

about 1 year (*Robock, 2000*). These sulphate aerosols heat the stratosphere by absorbing infra-red terrestrial radiation.

5. QBO Variability

The amorphous zone of QBO frequencies in figure 3 indicated the variable nature of the QBO. Here we characterise the QBO variability more precisely and investigate the form that this variability takes.

5.1 QBO Shear Zone Descent

Over the height range 15 hPa (~30 km) to 44 hPa (~22 km) the mean descent rate of the westerly shear zone is 4 hPa/month (standard deviation of 1.3 hPa/month) and the mean easterly shear zone descent rate is 2 hPa/month (standard deviation of 3.4 months). There is an occasional delay in the descent of the easterly shear zone (see figure 1a) when it stalls in the mid-stratosphere (~30 hPa) [*Dunkerton and Delisi, 1985; Naujokat, 1986; Swinbank and O'Neill, 1994; Salby and Callaghan, 2000*]. Two such stalling events can be found in 1965 and 1989. In both cases the descent of the easterly shear zone halted for over 8 months at 35 hPa before continuing its descent to the lower stratosphere. However, at other times there is little or no delay of the descent of the easterly shear zone, such as the years 1960, 1970 and 1998. This intermittent retardation of the easterly shear zone in the stalling region at approximately 30 hPa accounts for the slower mean descent rate of the easterly shear zone compared with the westerly shear zone. This variable behaviour of the easterly shear zone also explains the large standard deviation.

5.2 QBO Phase Transition and the Annual Cycle

The difference in variability between the east and west shear zone descent rates can be further illustrated by considering the timing of the east-west and west-east QBO phase transitions in the lower stratosphere. Figure 7 displays histograms of the timing of the onset of westerlies (E-W transitions) and easterlies (W-E transitions) grouped by month. At 44 hPa east-west phase transitions (figure 7c) occur throughout the year with a slight bias towards the month of June (21%), while west-east phase transitions (figure 7d) show a much stronger link to the annual cycle with 37% occurring in June. In the mid stratosphere, at 20 hPa, there is a smaller annual cycle in the opposite sense. The east-west phase transitions (figure 7a) show a bias towards December, when 32% of transitions occur, while the west-east transitions (figure 7b) are spread more evenly throughout the year.

Since east-west phase transitions at 20 hPa (figure 7a) show a bias towards December and the mean westerly shear zone descent rate is ~ 4 hPa/month, one would expect to see a corresponding transition bias 5-6 months later at 44 hPa during June. This is confirmed in figure 7c. West-east phase transitions at 20 hPa, above the stalling region (~ 30 hPa), occur throughout the year (figure 7b). Below the stalling region (~ 30 hPa) the 44hPa west-east phase transitions have a tendency to cluster about the months of May, June and July (figure 7d). This clustering appears to be achieved via variable retardation of the descending of the easterly shear zone.

The tendency for QBO phase transitions to become synchronised with the annual cycle has long been recognised [*Lindzen and Holton, 1968; Wallace, 1973; Dunkerton and Delisi, 1985; Dunkerton, 1990; Huesmann and Hitchman, 2001*]. More recently *Baldwin et al (2001)* found that 50 hPa west-east phase transitions in the NCEP reanalysis data set

were most likely to occur during April, May and June. The present analysis of the ERA-40 data (figure 7d) agrees well with these previous studies.

Kinnersley and Pawson (1996) have suggested that changes in the descent rate of the QBO are linked to the annual variation of the strength of Brewer-Dobson upwelling at the equator which is weakest during May, June and July. They suggest that the Brewer-Dobson upwelling acts to reinforce the residual upward circulation associated with the easterly QBO shear zone and thereby stalls its descent. Hence, whether or not an easterly shear zone becomes stalled should depend on the time of year in which the transition arrives above the stalling region. Our analysis supports this mechanism.

5.3 Solar Modulation of the QBO

Salby and Callaghan (2000) examined the duration of easterlies and westerlies in the lower equatorial stratosphere and found that the duration of the westerly phase of the QBO is more variable than the duration of the easterly phase. This result is consistent with the intermittent retardation of the descent of the easterly shear zone which consequently increases the duration of the westerly QBO in the lower stratosphere in some years and increases the standard deviation of both the easterly shear descent rate and the westerly phase duration. *Salby and Callaghan (2000)* found that the duration of the west phase of the QBO in the lower stratosphere varied systematically with solar activity such that long (short) periods of equatorial westerlies were coincident with minima (maxima) in solar activity.

Figure 8a shows a time series of the ERA-40 44 hPa equatorial zonal wind (the time series has been extended beyond 2001 with ECMWF operational data) which demonstrates a large variation of the duration of the westerly QBO phase. Figure 8b can

be used to assess the systematic variation in the duration of westerlies, it shows the duration of westerly and easterly equatorial zonal wind at 44 hPa superposed on a time series of the 10.7 cm Solar Radio Flux (a proxy for solar activity). From this we can observe an approximate 10 year periodicity in the duration of the westerly phase of the QBO which is generally out of phase with the solar cycle. This is in good agreement with the results of *Salby and Callaghan (2000)*.

The duration of westerlies in the lower stratosphere can be related to the rate of descent of the easterly QBO shear zone from the mid to lower stratosphere (15-44 hPa), shown in figure 8c. A slow or stalled descent of the easterly shear zone coincides with lengthy QBO westerlies in the lower stratosphere. Hence, the descent rate of the easterly shear zone also demonstrates periodic variation with a mean period (minima-minima) of 11 years. The longer period westerly phase during solar minimum periods found both here in the ERA-40 data and by *Salby and Callaghan (2000)* implies more stalling events in solar minimum years and figure 8c confirms this, with smaller easterly shear descent rates during solar minimum periods.

The easterly shear zone descent rate thus appears to follow the solar cycle with a lag of 14 months and the agreement is good up to 1990. A Spearson's rank correlation of easterly descent rate for the period from 1958 to 1990 versus a 12 month running mean of the solar radio flux has been calculated and the coefficient at a lag of 14 months is found to be 0.84. However, during the 1990's this correlation between the rate of easterly shear zone descent and the solar cycle seems to break down. The break down is particularly apparent for the 1997 easterly shear zone which one would have expected to stall had the relationship with the solar cycle been more robust. Instead, the easterly shear zone descends at a more or less constant rate from the mid to lower stratosphere (figure 1a).

Perhaps this steady descent is unsurprising since the west-east phase transition at 20 hPa occurs in November and so the easterly shear zone has just enough time to descend to 44 hPa for the favoured May-July period in 1998. However, the 1990's were an anomalous decade in terms of other atmospheric events which occurred in the tropics. The tropical climate in the early part of the decade was dominated by the eruption of Mt Pinatubo in June 1991 which was accompanied by changes in diabatic heating (figure 6) and tropical upwelling (*Salby and Callaghan, 2000*). The period from 1990 to 1994 saw a series of El Niño events which occurred in rapid succession (1991-1992, 1993 and 1994.) Latterly, in 1997, an El Niño developed whose strength exceeded any previously observed in the 20th century (*Slingo and Annamalai, 2000*). El Niño events are characterised by major shifts in the location and strength of tropical convection across the entire Pacific and most major monsoon regions of the world (*Bell and Halpert, 1998*). Such changes in convective activity could influence the QBO through changes in the gravity wave spectrum initiated by deep tropical convection. Such gravity waves are thought to be an important QBO driving mechanism (*Dunkerton, 1997*).

The ERA-40 time series of equatorial winds has been updated with the addition of ECMWF operational analyses to allow the interpretation of shear zone descent behaviour beyond the end of the 1990's. This additional data seems to indicate a resumption of the positive correlation between the descent rate of the easterly QBO shear zone and the solar cycle.

5.4 QBO – Solar Modulation Mechanism

There are several possible mechanisms for the solar modulation of the QBO period in the lower stratosphere. Following the mechanism proposed by *Kinnersley and Pawson*

(1996) that showed the QBO shear zone descent rates and period to be sensitive to the annual variation in the strength of the equatorial upwelling, there is the possibility that the 11-solar cycle introduces inter-annual variations in the strength of this upwelling.

The strength of the residual circulation is known to be influenced by the level of planetary wave activity in the winter hemisphere and there is observational evidence of a solar and QBO modulation of the winter-time polar vortex [e.g. *Labitzke and van Loon*, 1988; *Kodera*, 1995; *Baldwin et al.* 2001]. Analysis of rocketsonde data (*Gray et al.*, 2001a) and the ERA-40 dataset (figure 1) has highlighted that the equatorial QBO extends into the upper stratosphere. Model studies have shown the sensitivity of the winter polar vortex evolution to wind anomalies in this region of the atmosphere and it is therefore possible that the interaction of the solar cycle and QBO influences occur here (*Gray*, 2003; *McCormack*, 2003; *Matthes et al.*, 2004; *Gray et al.*, 2004) and then extends to the lower equatorial stratosphere via modulation of planetary wave propagation and the strength of the residual circulation.

In addition to the “polar” route of influence described above, there is an “equatorial” route which should also be considered. In figure 7 the east-west and west-east phase transition timings have also been annotated according to the phase of the solar cycle. A plus / minus annotation denotes a transition during solar maximum / minimum. Quite strikingly, all of the west-east phase transitions at 20 hPa (figure 7b) in solar maximum years occurred between October and January while in solar minimum years there is no preferred timing at 20 hPa. Since this preferred period in solar max is just before the May-July period when descent of the easterly shear zone is more rapid because of reduced upwelling, it is likely that the duration of the westerly phase in solar max years will be shorter, as observed. This is therefore an additional mechanism that could produce a solar

modulation of the QBO period in the lower stratosphere that does not involve a modulation of the equatorial upwelling via planetary wave modulation. It is not immediately obvious what mechanism produces the solar modulation of the equatorial QBO west-east phase transition at 20 hPa in figure 7b, although 20 hPa may be sufficiently high in the atmosphere to be impacted directly by changes in temperature distribution caused by the solar cycle (*Crooks and Gray, 2004*). It seems likely that both polar and equatorial routes of influence are important. Further modelling studies will be needed to determine which, if either, of the two mechanisms is the dominant one.

5.5 Cautionary Note (Other Possible Explanations)

The solar modulation of the QBO seems a fairly robust phenomenon. However, we must treat this connection with caution especially given the changing nature of the QBO-solar relationship observed in the 1990s. *Hamilton (2002)* cast some doubt on the connection between changes in solar irradiance and the period of the QBO suggested by *Salby and Callaghan (2000)*. While acknowledging that variations in the QBO period length were not random *Hamilton (2002)* suggested that a conclusive answer may need to await the availability of at least one or two more solar cycles.

Gray and Dunkerton (1990) have suggested that the slow modulation of the QBO could be related to the changing phase relationship of the QBO with the annual cycle. For instance a QBO with a constant period of 28 months would require 3 QBO cycles or 7 years to return to the initial phase relationship with the annual cycle. Similarly a QBO with a period of 26 months would require 6 cycles or 13 years. Although model experiments (*Crooks, pers. comm.*) do not appear to support this as a major factor, this possibility and other 'beating' mechanisms cannot be discounted as a contributory factor.

Another possible mechanism to describe the decadal QBO modulation has been presented in a modelling study by *Mayr et al.* (2003). This showed that beat periods between 9 and 11 years could be generated by the QBO as it interacts through gravity wave filtering with the semi-annual oscillation (SAO).

It has also been suggested that the diabatic heating due to volcanic aerosols could be responsible for the occasional suspension of the downward propagation of the QBO (*Dunkerton, 1983*). *Marquadt (1997)* showed that the downward phase propagation of the QBO can be blocked by forced diabatic heating when it is introduced in the easterly shear zone but found scarcely no change when the heating was introduced to westerly shear. Three major tropical volcanic eruptions occurred during the ERA-40 data period: Mt. Agung in Bali (March 1963), El Chichon in Mexico (April 1982) and Pinatubo (June 1991). Of these three eruptions only Pinatubo injected debris into the stratosphere during an easterly shear phase of the QBO. Mt. Agung and El Chichon both injected debris at the onset of westerly wind shear and so would not be expected to influence the downward phase propagation of the QBO. Hence, one would not expect the observed periodic retardation of the easterly QBO shear zone (figure 8c) to have come about as a result of volcanic activity alone.

6. Summary

The ERA-40 dataset confirms that the QBO exhibits large cycle to cycle variability with a mean period of 28.4 months and a standard deviation of 4 months. The westerly QBO shear zones descend more regularly and rapidly than easterly QBO shear zones. Mean westerly shear zone descent rate is 4 hPa/month with a standard deviation of 1.3 months.

Mean easterly shear zone descent rate is 2 hPa/month with a standard deviation of 3.4 months.

The ERA-40 dataset has also revealed that the QBO exhibits a three fold vertical phase structure. In addition to the well-known 2-fold structure in the lower and mid stratosphere, e.g. easterlies overlying westerlies or vice versa, there is a third anomaly in the upper stratosphere. The sign of this upper stratospheric anomaly is the same as the lower stratospheric anomaly, thus forming anomalies of alternating sign throughout the depth of the equatorial stratosphere. The difference between west and east QBO composites (figure 5c) is $+30 \text{ ms}^{-1}$ at 23 km, -25 ms^{-1} at 35 km and $+10 \text{ ms}^{-1}$ at 48 km.

There is a tendency for a seasonal preference in the timing of the west-east QBO phase transition in the lower stratosphere (44 hPa). 37% of west-east phase transitions occur in June. There is also a strong indication of a connection between the descent rate of the easterly QBO shear zone and the solar cycle. In the mid-stratosphere (20 hPa) all solar maximum west-east QBO phase transitions occur during Northern Hemisphere winter (October to January). The timing of this phase transition ensures that the easterly shear zone arrives in the stalling region (~ 30 hPa) during Northern Hemisphere summer (May to July) when Brewer-Dobson upwelling is weakest. The easterly shear zone can then descend to the lower stratosphere without hindrance. The mean time required for easterly shear zones to descend from 20 hPa to 44 hPa is 2 months less during solar maxima than during solar minima (7.4 months versus 9.7 months). The rapid descent of easterly shear zones during periods of solar maxima cuts short the west phase of the QBO in the lower stratosphere as noted by *Salby and Callaghan* (2000). Whether this solar modulation is via a ‘polar route’ in which it is a result of the solar modulation of the Brewer-Dobson upwelling via planetary wave modulation, or whether it is via an ‘equatorial route’ in

which solar modulation directly affects the equatorial temperature and winds at 20 hPa requires further evaluation and modelling.

Acknowledgements

We would like to thank the British Atmospheric Data Centre (BADC) who kindly provided the ERA-40 data and also the National Geophysical Data Centre (NGDC) from whom we obtained the solar radio flux observations. We would also like to acknowledge the Natural Environment Research Council (NERC) who funded this work.

References

- Angell, J. K., and J. Korshover, Quasi-biennial variations in temperature, total ozone, and tropopause height, *J. Atmos. Sci.*, 21, 479-492, 1964.
- Baldwin, M. P., L. J. Gray, T. J. Dunkerton, K. Hamilton, P. H. Haynes, W. J. Randel, J. R. Holton, M. J. Alexander, I. Hirota, T. Horinouchi, D. B. A. Jones, J. s. Kinnersley, C. Marquardt, K. Sato and M. Takahasi, The Quasi-Biennial Oscillation, *Reviews of Geophysics*, 39, 179-229, 2001.
- Baldwin, M. P., and T. J. Dunkerton, Quasi-biennial oscillation above 10mb, *Geophysical Research Letters*, 18(7), 1205-1208, 1991.
- Bell, G. D., and M. S. Halpert, Climate assessment for 1997, *Bulletin of the American Meteorological Society*, 79(5), S1-S50, 1998.
- Crooks, S. A., and L. J. Gray, Characterisation of the 11-year solar signal using a multiple regression analysis of the ERA-40 dataset, *submitted to Journal of Climate*, 2004.
- Dunkerton, T. J., Modification of stratospheric circulation by trace constituent changes?, *J. Geophys. Res.*, 88, 10,831-10,836, 1983.
- Dunkerton, T. J., Annual variation of deseasonalized mean flow acceleration in the equatorial lower stratosphere, *J. Meteorol. Soc. Jpn.*, 68, 499-508, 1990.
- Dunkerton, T. J., The role of gravity waves in the quasi-biennial oscillation, *J. Geophys. Res.* 102(D22), 26,053-26,076, 1997.
- Dunkerton, T. J., and M. P. Baldwin, Quasi-biennial modulation of planetary wave fluxes in the Northern hemisphere winter, *J. Atmos. Sci.*, 48(8), 1043-1061, 1991.

Dunkerton, T. J., and D. P. Delisi, Climatology of the equatorial lower stratosphere, *J. Atmos. Sci.*, 42, 376-396, 1985.

Ebdon, R. A., Notes on the wind flow at 50 mb in tropical and subtropical regions in January 1957 and in 1958, *Q. J. R. Meteorol. Soc.*, 86, 540-542, 1960.

Gray, L. J., The influence of the equatorial upper stratosphere on stratospheric sudden warmings, *Geophys. Res. Lett.*, 30, doi:10.1029/2002GL016430, 2003.

Gray, L. J., S. A. Crooks, C. L. Pascoe, S. Sparrow and M.A. Palmer, Solar and QBO influences on the timing of stratospheric sudden warmings, 2004.

Gray, L. J., E. F. Drysdale, T. J. Dunkerton, and B. N. Lawrence, Model studies of the interannual variability of the northern-hemisphere stratospheric winter circulation: The role of the quasi-biennial oscillation, *Q. J. R. Meteorol. Soc.*, 127, 1413-1432, 2001a.

Gray, L. J., and T. J. Dunkerton, The role of the seasonal cycle in the quasi-biennial oscillation of ozone, *J. Atmos. Sci.*, 47(20), 2429-2451, 1990.

Gray, L. J., S. J. Phipps, T. J. Dunkerton, M. P. Baldwin, E. F. Drysdale, and M. R. Allen, A data study of the influence of the equatorial upper stratosphere on northern-hemisphere stratospheric sudden warmings, *Q. J. R. Meteorol. Soc.*, 127, 1985-2003, 2001b.

Hamilton, K., On the quasi-decadal modulation of the stratospheric QBO period, *Journal of Climate*, 15, 2562-2565, 2002.

Hitchman, M. H., E. Kudeki, D. C. Fritts, J. M. Kugi, C. Fawcett, G. A. Postel, C. Y. Yao, D. Ortland, D. Riggin, and V. L. Harvey, Mean winds in the tropical stratosphere and

- mesosphere during January 1993, March 1994, and August 1994, *J. Geophys. Res.*, *102*, 26,033-26,052, 1997.
- Holton, J.R. and R.S. Lindzen, An updated theory for the quasi biennial oscillation of the tropical stratosphere, *J. Atmos. Sci.*, *29*, 1076-1080, 1972.
- Huesmann, A. S., and M. H. Hitchman, The stratospheric quasi-biennial oscillation in the NCEP reanalyses: Climatological structures. *J. Geophys. Res.*, *106*, 11,859-11,874, 2001.
- Kinnersley, J. S., and S. Pawson, The descent rates of the shear zones of the equatorial QBO. *J. Atmos. Sci.*, *53(14)*, 1937-1949, 1996.
- Kodera, K., On the origin and nature of the interannual variability of the winter stratospheric circulation in the northern hemisphere., *J. Geophys. Res.*, *100(D7)*, 14077-14087, 1995.
- Labitzke, K., and H. van Loon, Associations between the 11-year solar cycle, the QBO and the atmosphere. Part I: the troposphere and stratosphere in the northern hemisphere in winter. *Journal of Atmospheric and Terrestrial Physics*, *50(3)*, 197-206, 1988.
- Lindzen, R. S., and J. R. Holton, A theory of the quasi-biennial oscillation, *J. Atmos. Sci.*, *25*, 1095-1107, 1968.
- Marquadt, C., Die tropische QBO und dynamische Prozesse in der Stratosphaere, Ph.D. Thesis published in *Meteorologische Abhandlungen*, Serie A, Band 9, Heft 4, Freie Universitaet Berlin, ISSN 0342-4324, 1997.
- Matthes, K., U. Langematz, L. J. Gray, K. Kodera, and K. Labitzke, Improved 11-year solar signal in the FUB-CMAM., *J. Geophys. Res.*, *109*, D06101, doi:10.1029/2003JD004012, 2004.

- Mayr, H. G., J. G. Mengel, D. P. Drob, H. S. Porter, and K. L. Chan. Modeling studies with QBO: I. Quasi-decadal oscillation. *Journal of Atmospheric and Solar Terrestrial Physics*, 65(8), 887-899, 2003.
- McCormack, J. P., The influence of the 11-year solar cycle on the quasi-biennial oscillation. *Geophys. Res. Lett.*, 30(22), 2162, doi:10.1029/2003GL018314, 2003.
- McCormick, M. P., and R. E. Veiga, SAGEII measurements of early Pinatubo aerosols, *Geophys. Res. Letts.*, 19, 155-158, 1992.
- Naujokat, B., An update of the observed quasi-biennial oscillation of the stratospheric winds over the tropics, *J. Atmos. Sci.*, 43, 1873-1877, 1986.
- Randel, W. J., E. Fleming, M. Geller, M. Gelman, K. Hamilton, D. Karoly, D. Ortland, S. Pawson, R. Swinbank, P. Udelhofen, M. Baldwin, M. L. Chanin, P. Keckhut, K. Labitzke, E. Remsberg, A. Simmons, and D. Wu, The SPARC Intercomparison of Middle Atmosphere Climatologies, WCRP-116, WMO/TD-1142, 2002.
- Randel, W. J., F. Wu, R. Swinbank, J. Nash, and A. O'Neil, Global QBO circulation derived from UKMO stratospheric analyses, *J. Atmos. Sci.*, 56(4), 457-474, 1999.
- Reed, R. J., W. J. Campbell, L. A. Rasmussen, and R. G. Rogers, Evidence of a downward propagating annual wind reversal in the equatorial stratosphere, *J. Geophys. Res.*, 66, 813-818, 1961.
- Robock, A., Volcanic eruptions and climate, *Reviews of Geophysics*, 38(2), 191-219, 2000.
- Salby, M., and P. Callaghan, Connection between the solar cycle and the QBO: The missing link. *Journal of Climate*, 13, 2652-2662, 2000.

Slingo, J. M., and H. Annamalai, The El Nino of the century and the response of the *Indian summer monsoon*. *Monthly Weather Review*, 128(6), 1778-1797, 2000.

Swinbank, R., and A. O'Neill, Quasi-biennial and semiannual oscillations in equatorial wind fields constructed by data assimilation. *Geophys. Res. Lett.*, 21(19), 2099-2102, 1994.

Tanni, R., and F. Hasebe, Ozone feedback stabilizes the quasi-biennial oscillation against volcanic perturbations, *Geophysical Research Letters*, 29(7), article 14, 2002.

Wallace, J. M., General circulation of the tropical lower stratosphere, *Rev. Geophys.*, 11,191-222, 1973.

QBO W				
1960	1962	1964	1965	1967
1970	1972	1974	1976	1979
1981	1983	1986	1988	1989
1991	1993	1998	2000	
QBO E				
1959	1961	1963	1966	1969
1971	1973	1975	1977	1978
1980	1982	1985	1990	1992
1997	1999			

Table 1.

QBO west and QBO east years listed according to the year in which the January of the December-January average falls.

Figure 1.

Zonally averaged monthly-mean equatorial zonal wind as a function of time and pressure. Easterlies are shown shaded. **(a)** Time-height section of the equatorial monthly-mean zonal wind component (contour interval: 10ms^{-1}). **(b)** Same as for a) but with the seasonal cycle removed (contour interval: 10ms^{-1}). **(c)** Same as for b) after application of a 9-48 month digital band-pass filter (contour interval: 5ms^{-1}). Ticks on the time-axis indicate January.

Figure 2.

Annual cycle of equatorial zonal mean zonal wind (1979-2001). Contour interval is 3ms^{-1} , easterly winds are shaded.

Figure 3.

Fourier analysis of equatorial zonal mean zonal wind. The frequency axis indicates the number of cycles that a periodic mode achieves during the 44 years of the ERA-40 dataset. Contours are drawn at Fourier amplitudes of 1, 2, 4, 8 and 16ms^{-1} .

Figure 4.

Amplitude of the QBO (ms^{-1}) calculated using Fourier analysis of the zonal mean zonal wind. The QBO amplitude is a function of the ratio of the power of QBO harmonics 13-24 to the power of all harmonics. This ratio is then multiplied by a measure of the amplitude of zonal wind variability given by H^2 times the rms of the zonal wind. **(a)** QBO amplitude, contours are drawn at 1, 4, 8, 12, 16 and 20ms^{-1} . **(b)** Vertical profile of the equatorial QBO. **(c)** Latitudinal profile of the QBO at 30 hPa. The solid profiles in figures b) and c) show the QBO amplitude calculated using the Fourier power spectrum and the broken profiles show the 'Equivalent QBO Amplitude'.

Figure 5.

The mean December January zonal mean zonal wind for QBO west **(a)** and QBO east **(b)** years. Easterly zonal mean wind is shown shaded and contours are at 10ms^{-1} intervals. **(c)**

West minus east zonal wind difference with T-test confidence shading shown at 95% and 99%, contours are at 5 ms^{-1} intervals.

Figure 6.

Equatorial zonal mean deseasonalised temperature anomalies (K) for the period 1958-2002 at 30 hPa (solid) and the vertical wind shear ($\text{m s}^{-1} \text{ km}^{-1}$) in the 30 to 55 hPa layer (broken).

Figure 7.

Histograms of the timing of the onset of westerlies at 44h Pa **(a)**, easterlies at 44 hPa **(b)**, westerlies at 20 hPa **(c)** and easterlies at 20 hPa **(d)**. Individual years are listed. Transition events marked with a plus occurred during solar maxima and those marked with a minus occurred during solar minima. Intermediate years have no extra annotation.

Figure 8.

(a) Time series of ERA-40 and ECMWF operational 44 hPa equatorial monthly-mean zonal wind (m s^{-1}). **(b)** Time series of the duration of east (broken) and west (heavy-solid) phases of the QBO at 44 hPa and the monthly mean solar radio flux ($\times 10^{-23} \text{ W m}^{-2} \text{ Hz}^{-1}$). **(c)** The rate of descent of the onset of easterlies from the mid to lower stratosphere (15-44 hPa) are shown by a heavy line, crosses mark the timing of the W-E transition at 15 hPa. The monthly mean solar radio flux ($\times 10^{-23} \text{ W m}^{-2} \text{ Hz}^{-1}$) is shown by a thin line.

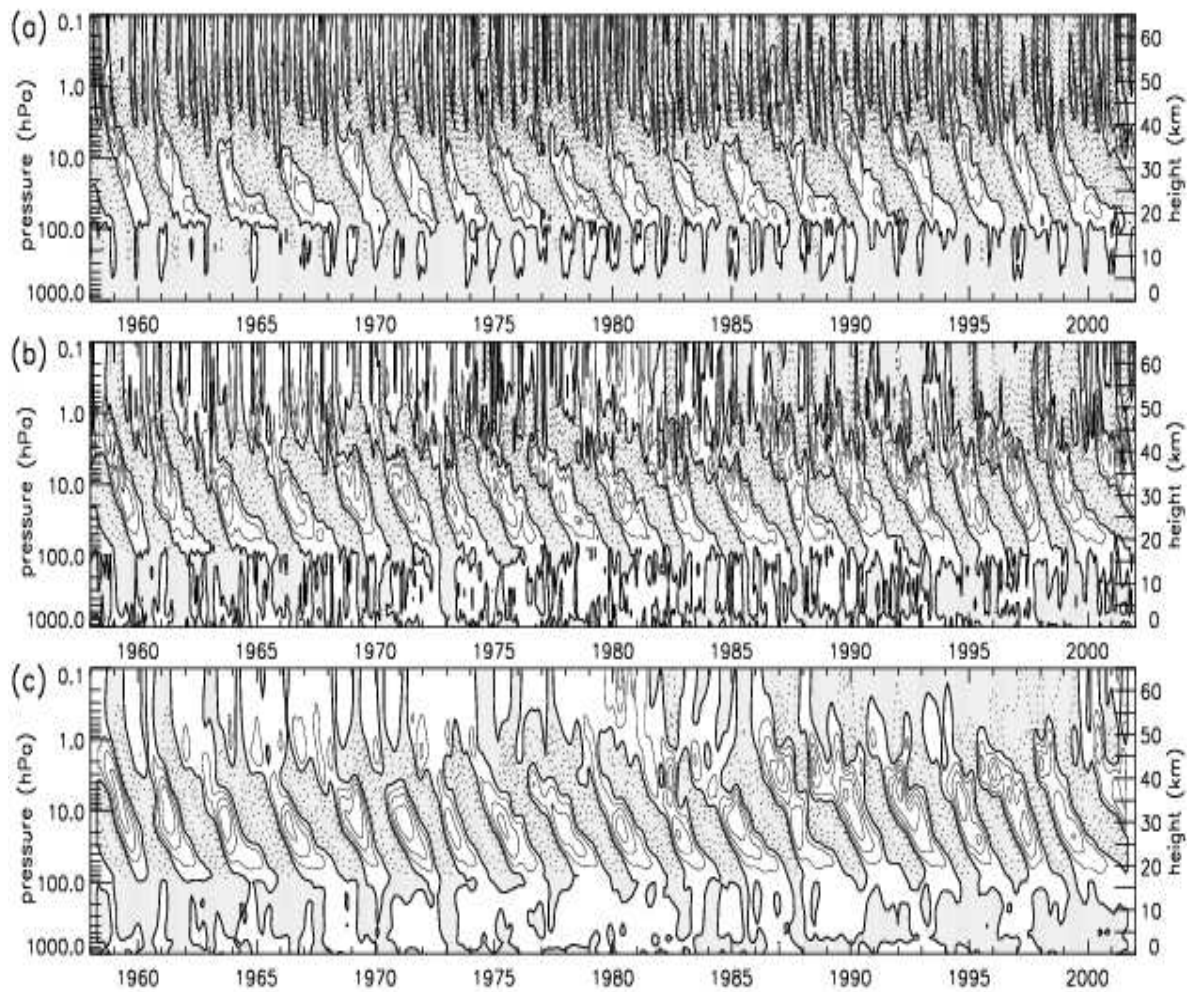


Figure 1

Zonally averaged monthly-mean equatorial zonal wind as a function of time and pressure. Easterlies are shown shaded. **(a)** Time-height section of the equatorial monthly-mean zonal wind component (contour interval: 10ms^{-1}). **(b)** Same as for a) but with the seasonal cycle removed (contour interval: 10ms^{-1}). **(c)** Same as for b) after application of a 9-48 month digital band-pass filter (contour interval: 5ms^{-1}). Ticks on the time-axis indicate January.

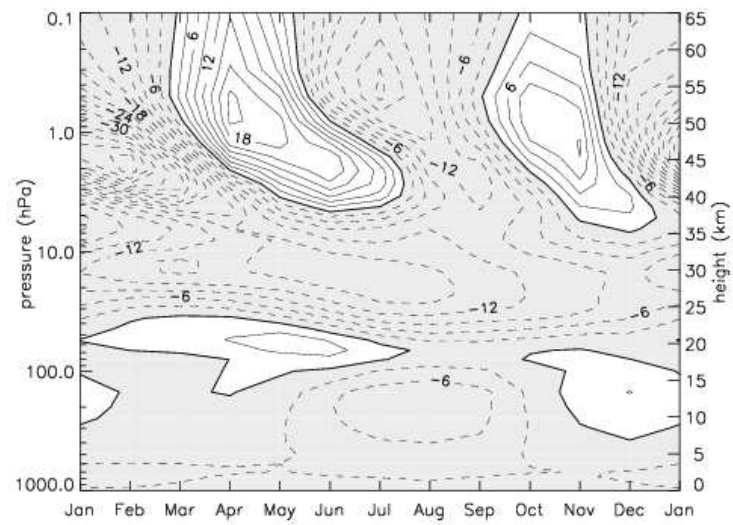


Figure 2

Annual cycle of equatorial zonal mean zonal wind (1979-2001). Contour interval is 3 ms^{-1} , easterly winds are shaded.

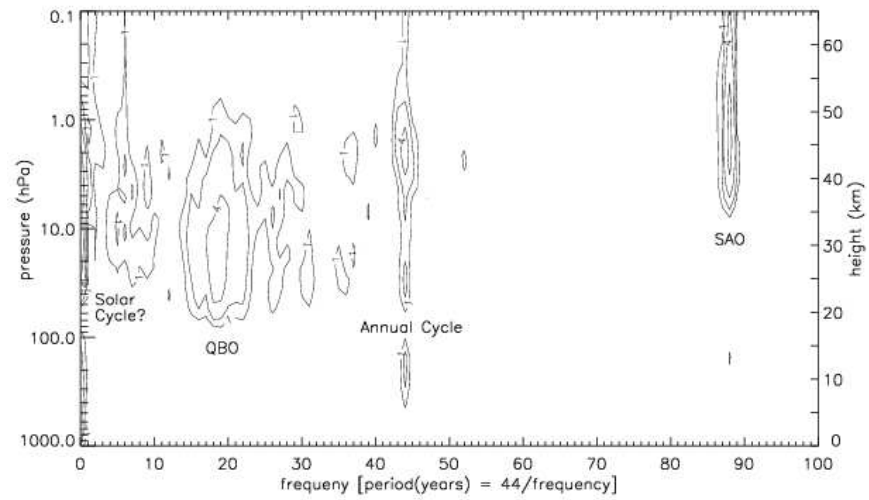


Figure 3

Fourier analysis of equatorial zonal mean zonal wind. The frequency axis indicates the number of cycles that a periodic mode achieves during the 44 years of the ERA-40 dataset. Contours are drawn at Fourier amplitudes of 1, 2, 4, 8 and 16 ms⁻¹.

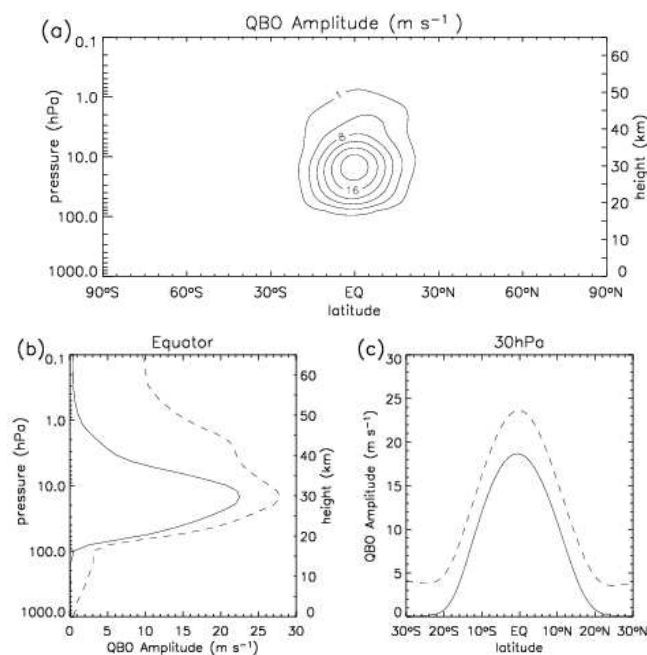


Figure 4

Amplitude of the QBO (ms^{-1}) calculated using Fourier analysis of the zonal mean zonal wind. The QBO amplitude is a function of the ratio of the power of QBO harmonics 13-24 to the power of all harmonics. This ratio is then multiplied by a measure of the amplitude of zonal wind variability given by $\sqrt{2}$ times the rms of the zonal wind. (a) QBO amplitude, contours are drawn at 1, 4, 8, 12, 16 and 20 ms^{-1} . (b) Vertical profile of the equatorial QBO. (c) Latitudinal profile of the QBO at 30 hPa. The solid profiles in figures b) and c) show the QBO amplitude calculated using the Fourier power spectrum and the broken profiles show the 'Equivalent QBO Amplitude'.

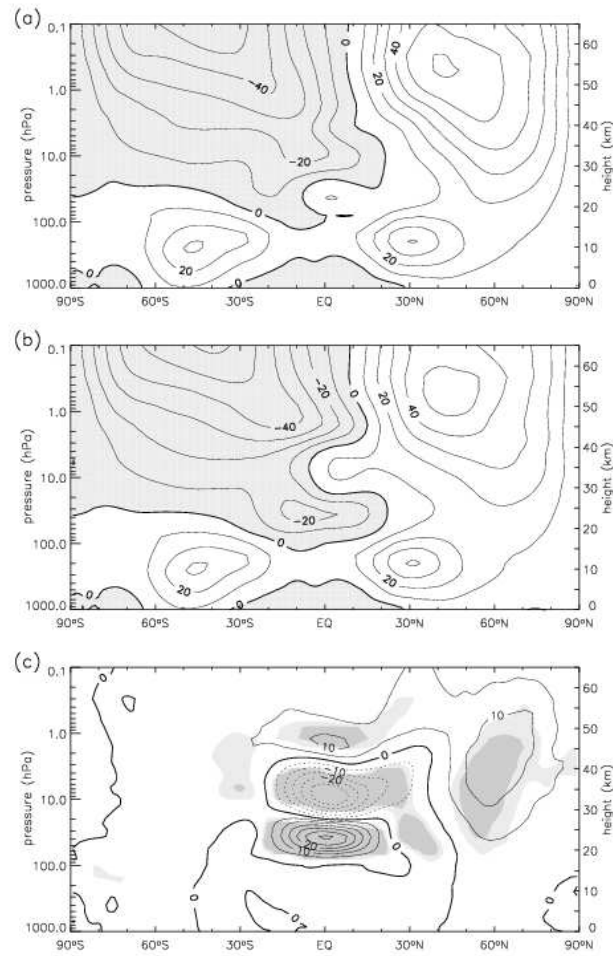


Figure 5

The mean December January zonal mean zonal wind for QBO west **(a)** and QBO east **(b)** years. Easterly zonal mean wind is shown shaded and contours are at 10 ms^{-1} intervals. **(c)** West minus east zonal wind difference with T-test confidence shading shown at 95% and 99%, contours are at 5 ms^{-1} intervals.

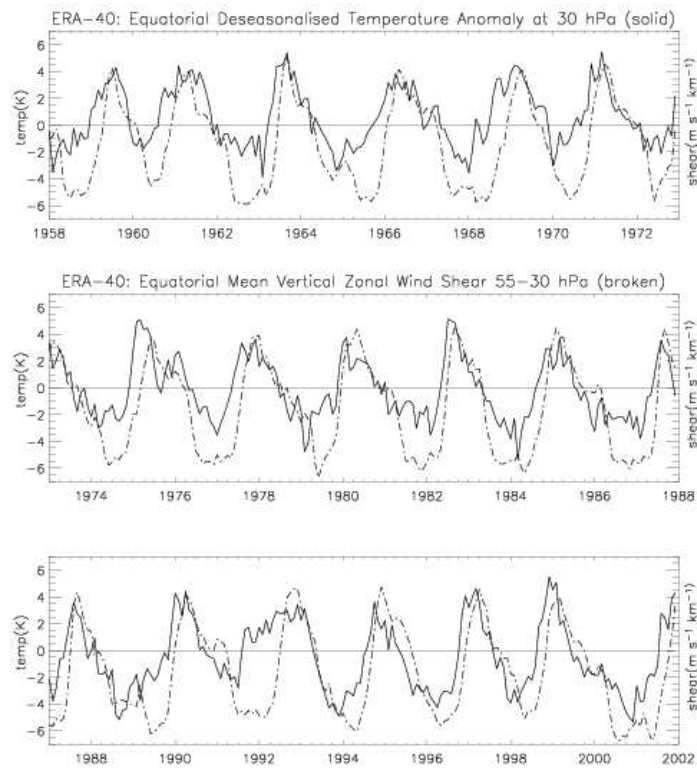


Figure 6

Equatorial zonal mean deseasonalised temperature anomalies (K) for the period 1958-2002 at 30 hPa (solid) and the vertical wind shear ($\text{m s}^{-1} \text{ km}^{-1}$) in the 30 to 55 hPa layer (broken).

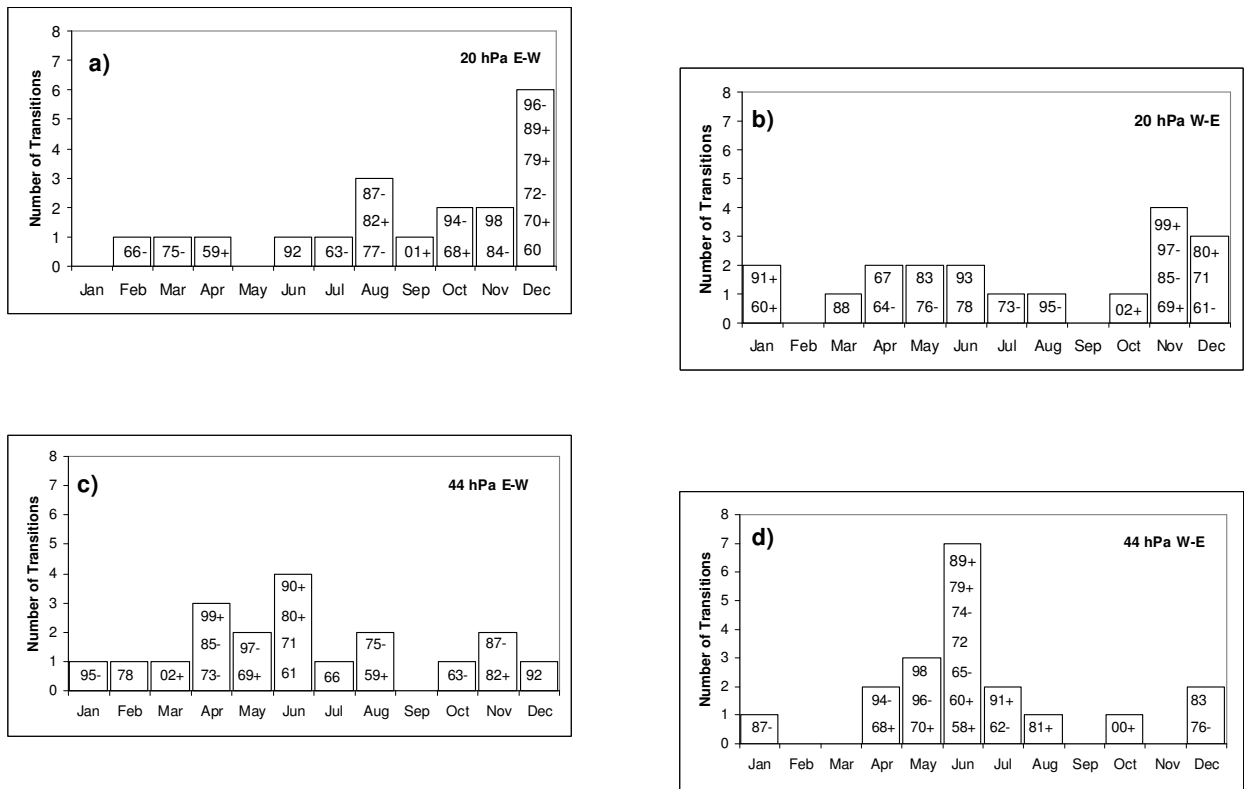


Figure 7

Histograms of the timing of the onset of westerlies at 20h Pa **(a)**, easterlies at 20 hPa **(b)**, westerlies at 44 hPa **(c)** and easterlies at 44 hPa **(d)**. Individual years are listed. QBO phase transition events marked with a plus occurred during solar maxima and those marked with a minus occurred during solar minima. QBO phase transition events which occurred during intermediate periods of the solar cycle have no extra annotation.

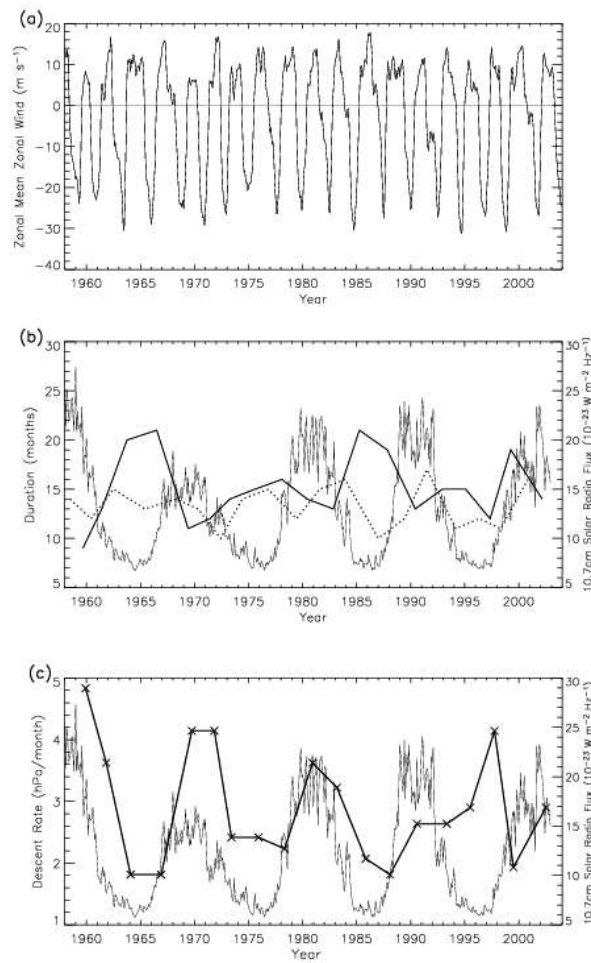


Figure 8

(a) Time series of ERA-40 and ECMWF operational 44 hPa equatorial monthly-mean zonal wind (m s^{-1}). (b) Time series of the duration of east (broken) and west (heavy-solid) phases of the QBO at 44 hPa and the monthly mean solar radio flux ($\times 10^{-23} \text{ W m}^{-2} \text{ Hz}^{-1}$). (c) The rate of descent of the onset of easterlies from the mid to lower stratosphere (15-44 hPa) are shown by a heavy line, crosses mark the timing of the W-E transition at 15 hPa. The monthly mean solar radio flux ($\times 10^{-23} \text{ W m}^{-2} \text{ Hz}^{-1}$) is shown by a thin line.

